

## Electronic Supplementary Information

---

# Thermodynamics of halogen bonded monolayer self-assembly at the liquid-solid interface

W. Song,<sup>a,b</sup> N. Martsinovich,<sup>d</sup> W. M. Heckl,<sup>a,b,c</sup> and M. Lackinger<sup>a,b,c</sup>

<sup>a</sup> Department of Physics, Technische Universität München, James-Frank-Str. 1, 85748 Garching, Germany.

<sup>b</sup> Nanosystems-Initiative-Munich & Center for NanoScience (CeNS), Schellingstr. 4, 80799 Munich, Germany.

<sup>c</sup> Deutsches Museum, Museumsinsel 1, 80538 Munich, Germany.

<sup>d</sup> Department of Chemistry, University of Sheffield, Sheffield S3 7HF, U.K.

*Tel: +49 89 2179-605; E-mail markus@lackinger.org*

### Table of content

1	Experimental details .....	2
1.1	STM experiments .....	2
1.2	Sublimation enthalpy measurement .....	3
1.3	Dissolution enthalpy measurement.....	3
2	Additional STM data .....	4
2.1	Split image.....	4
2.2	Overview image.....	5
3	Entropy estimation.....	7
3.1	Translational entropy.....	7
3.2	Rotational entropy .....	8
4	Density Functional Theory .....	9
4.1	Calculational Details .....	9
4.2	Additional results.....	11
5	References .....	12

# 1 Experimental details

2,3,6,7,10,11-Hexabromotriphenylene (HBTP) was purchased from TCI Europe N.V. with a purity of >98%. 1-Heptanoic acid (7A) was purchased from Sigma-Aldrich with a purity of  $\geq 99\%$ . Both compounds were used as received without further purification.

## 1.1 STM experiments

Scanning Tunneling Microscopy (STM) experiments were conducted with a home-built low-drift instrument operated with a commercial ASC500 control electronics (attocube Systems AG, Munich). Highly Oriented Pyrolytic Graphite (ZYB grade, Optigraph GmbH, Berlin) was used and freshly cleaved prior to each experiment. Images were acquired directly at the liquid-solid interface with mechanically cut Pt/Ir tips. To avoid inaccuracies in the concentration dependent experiments due to spilling of solution or solvent evaporation, a rimmed sample holder was used with a relatively high solution volume ( $\sim 40 \mu\text{L}$ ).

The critical concentration  $c_{\text{crit}}$  was determined by probing solutions with different concentrations in STM experiments. The samples were obtained by diluting a stock solution prepared from  $3.41 \text{ mg} \pm 0.10 \text{ mg}$  HBTP and  $10.0 \text{ mL}$  heptanoic acid, corresponding to a concentration of  $486 \mu\text{mol/L}$ . The relative volume error for the dilution is estimated as 4 %. Accordingly, the total concentration error related to solution preparation amounts to  $\sim 7 \%$ .

In the STM experiments full monolayer coverage was still observed for a concentration of  $30.4 \mu\text{mol/L}$ , whereas no adsorbed structures could be discerned anymore for a concentration of  $27.0 \mu\text{mol/L}$ . Using a concentration of  $30.4 \mu\text{mol/L}$  the self-assembled monolayer could be imaged in less than one minute. Consequently, slow kinetics is ruled out as a possible reason for the absence of self-assembled structures at the slightly lower concentration of  $27.0 \mu\text{mol/L}$ . Taking the above discussed concentration uncertainty of  $\sim 7 \%$  into account results in an upper and

lower boundary for  $c_{\text{crit}}$  of 32.5  $\mu\text{mol/L}$  and 25.1  $\mu\text{mol/L}$ , respectively. For evaluation of translational entropy the average value of 28.8  $\mu\text{mol}$  was used, and in the manuscript an error margin of  $\pm 3.7 \mu\text{mol/L}$  was stated.

## 1.2 Sublimation enthalpy measurement

The sublimation enthalpy  $\Delta H_{\text{cryst} \rightarrow \text{vac}}$  was derived from the temperature dependence of the HBTP vapour pressure by applying the Van't Hoff equation. The vapour pressure of a compound is in good approximation proportional to its effusion rate from a Knudsen cell (a vacuum sublimation deposition source). Effusion rates were measured with a quartz crystal microbalance (QCMB, crystal diameter 1.4 cm, nominal eigenfrequency 6.0 MHz) for different crucible temperatures in a high-vacuum chamber at  $\sim 10^{-7}$  mbar. A home-built Knudsen cell was used,<sup>1</sup> where the crucible temperature was measured with a type K thermocouple and held constant with a Eurotherm 2416 temperature controller (Invensys Systems GmbH, Limburg an der Lahn). A commercial Q-pod thickness monitor (Inficon) was used to drive and readout the QCMB. The crucible temperature was varied between 225 °C and 270 °C (increment 5 °C). In all cases the  $\Delta f$  vs.  $t$  traces were perfectly linear, indicating a stable and constant effusion rate. The resulting Van't Hoff plot is also perfectly linear, thereby confirming the validity of the chosen approach.

## 1.3 Dissolution enthalpy measurement

The dissolution enthalpy  $\Delta H_{\text{cryst} \rightarrow \text{sol}}$  was derived from the temperature dependence of the HBTP solubility in 7A by applying the Van't Hoff equation. The solubility was measured by UV-Vis absorption spectroscopy of saturated solutions for temperatures between 22 °C and 54 °C (increment 3 °C). According to the Lambert-Beer law the absorbance is a measure for the concentration of the absorbing compound. To avoid inaccuracies due to temperature dependent

changes in the overall shape of the UV-Vis absorption spectra, the total absorbance was obtained by integration over the absorption band from  $\lambda = (270 \text{ .. } 340) \text{ nm}$ .

The experimental setup consists of an ISS-UV-Vis light source combined with an USB4000 optical spectrometer (Ocean Optics). A quartz glass cuvette with 10 mm optical path length was used which was heated by two sideways mounted Peltier elements (TEC1-03504). The solution temperature was measured directly in the cuvette by an immersed type K thermocouple and held constant with a Eurotherm 2416 temperature controller. UV-Vis absorption spectra were acquired only after an equilibration time of 24 h when a new temperature was adjusted. UV-Vis absorption spectra of pure 7A solvent at the respective temperature served as references. Similarly, this approach results in a perfectly linear Van't Hoff plot.

## 2 Additional STM data

### 2.1 Split image

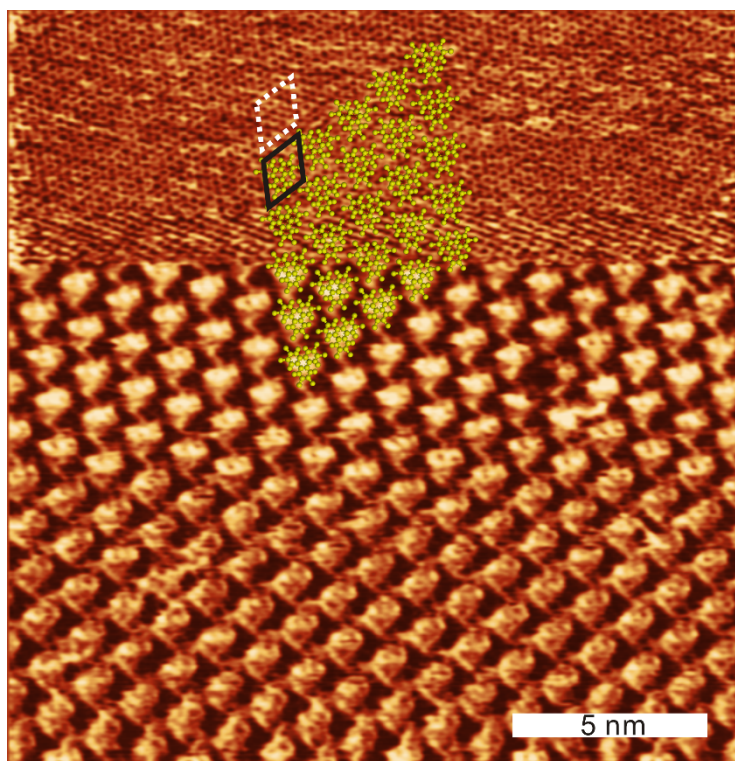


**Fig. S1.** High-resolution STM image of a HBTP monolayer acquired at the 7A-graphite interface. In the lower part, the HBTP superstructure was imaged with typical tunneling parameters of  $V_{\text{sample}} = -300$  mV,  $I = 60$  pA. In the upper part, the tunneling resistance was reduced by two orders of magnitude through switching the tunneling voltage to  $-3.0$  mV. Consequently, the underlying graphite substrate could be imaged with atomic resolution. This so called “split-image” reveals an alignment of the graphite with the HBTP lattice vectors. The black rhombus indicates the HBTP unit cell. The white dashed rhombus also indicates the HBTP unit cell, but has been laterally shifted to illustrate the alignment between HBTP and graphite lattice vectors.

---

## 2.2 Overview image

---

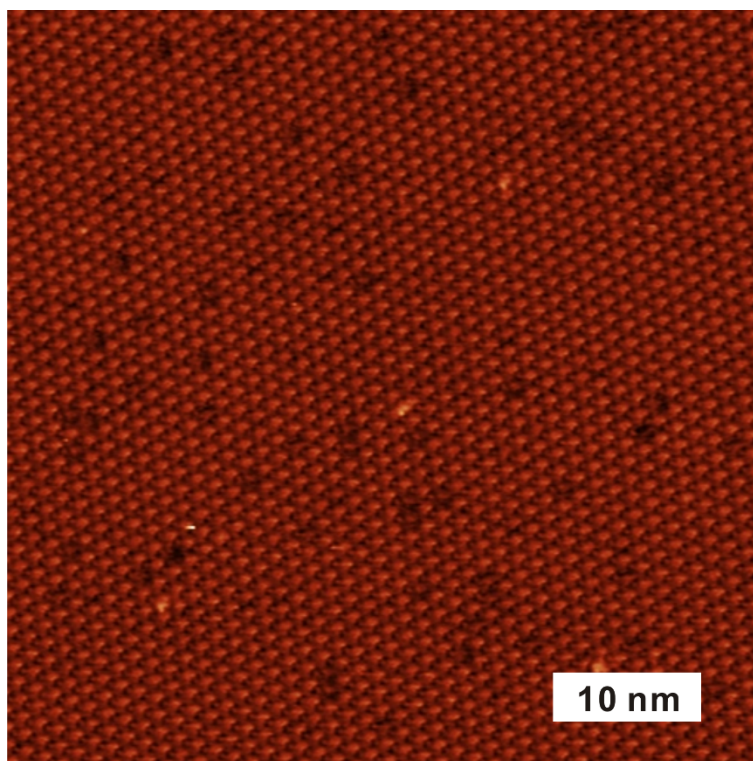


**Fig. S2.** Overview STM image of a HBTP monolayer acquired at the 7A–graphite interface ( $V_{\text{sample}} = -200$  mV,  $I = 60$  pA). The monolayer appears with uniform STM contrast. The absence

of a periodic contrast modulation, i.e. a Moiré pattern, indicates similar adsorption sites of all HBTB molecules in a commensurate superstructure.

---

### 3 Entropy estimation

The total entropy change  $\Delta S$  of monolayer self-assembly is partitioned into translational, rotational, vibrational, and conformational entropy as proposed by Whitesides et al.,<sup>2</sup> and as similarly applied in previous studies.<sup>3, 4</sup> Since HBTP is a rigid molecule without rotatable bonds, conformational entropy is not further considered. Also vibrational entropy does not significantly change upon supramolecular self-assembly, and can hence similarly be neglected. The dominant contributions to  $\Delta S$  arise from changes in translational entropy  $\Delta S_{\text{trans}}$  and rotational entropy  $\Delta S_{\text{rot}}$ . Both  $S_{\text{trans}}$  and  $S_{\text{rot}}$  are relatively small in the adsorbed state as compared to the dissolved state, and are hence assumed to be zero within the monolayer. Accordingly, the total entropy is obtained from  $\Delta S = \Delta S_{\text{rot}} + \Delta S_{\text{trans}} = S_{\text{rot(adsorbed)}} - S_{\text{rot(sol)}} + S_{\text{trans(adsorbed)}} - S_{\text{trans(sol)}} = 0 - S_{\text{rot(sol)}} + 0 - S_{\text{trans(sol)}} = - [S_{\text{rot(sol)}} + S_{\text{trans(sol)}}]$ , whereby  $S_{\text{rot(sol)}}$  and  $S_{\text{trans(sol)}}$  refer to entropies of HBTP in solution. In other words,  $\Delta S$  is estimated as the sum of translational and rotational entropy of HBTP molecules in solution.

#### 3.1 Translational entropy

Translational entropy was evaluated by the Sackur-Tetrode equation:

$$S_{\text{trans(sol)}} = - R \ln \left[ \frac{1}{c} \left( \frac{2\pi m k_B T e^{5/3}}{h^2} \right)^{3/2} \right] \quad (1)$$

R is the gas constant, c the solute concentration, T the temperature,  $k_B$  the Boltzmann constant, h Planck's constant, e Euler's number, and m the absolute mass of a HBTP molecule. The Sackur-Tetrode equation was originally derived for gases. To avoid overestimation of translational entropy in solution free volume corrections were applied. Moreover, it is assumed that all 7A

solvent molecules are dimerized in the liquid phase. The free volume  $V_{free}$  of the 7A solvent was estimated with the hard cube approximation:<sup>2</sup>

$$V_{free} = 8(\sqrt[3]{V_{ave}} - \sqrt[3]{V_{molec}})^3$$

$V_{ave}$  is the average available volume of a 7A-7A dimer in the liquid phase,  $V_{molec}$  corresponds to its van der Waals volume. With a mass density of 7A solvent of  $0.92 \text{ g}\cdot\text{cm}^{-3}$  and a van der Waals volume of  $278.6 \text{ \AA}^3$  per 7A dimer,  $V_{free}$  is estimated as  $32.6 \text{ mL}$  per liter 7A. This free volume correction can also be viewed as an apparent concentration enhancement by a factor of  $\sim 31$ . For the numerical evaluation of  $S_{\text{trans(sol)}}$  the experimentally derived critical concentration of  $28.8 \mu\text{mol L}^{-1}$  and a temperature of  $T=298 \text{ K}$  were used, resulting in  $S_{\text{trans(sol)}} = \Delta S_{\text{trans}} = -222.3 \text{ J}\cdot\text{mol}^{-1}\cdot\text{K}^{-1}$ . Owing to the logarithmic dependence of  $S_{\text{trans}}$  on  $c$ , the experimental uncertainty in  $c_{\text{crit}}$  of  $\pm 3.7 \mu\text{mol/L}$  results in a negligibly small uncertainty of  $\sim 1 \text{ J}\cdot\text{mol}^{-1}\cdot\text{K}^{-1}$  in  $S_{\text{trans}}$  that is not further considered.

### 3.2 Rotational entropy

Rotational entropy was estimated using the rigid rotator model:

$$S_{rot(sol)} = -R \ln \left[ \frac{\pi^{1/2} (8\pi^2 k_B T e)}{\gamma h^2} \right]^{3/2} (I_1 I_2 I_3)^{1/2} \quad (2)$$

$I_1$ ,  $I_2$ , and  $I_3$  are the principal moments of inertia of a HBTP molecule.  $\gamma$  is the symmetry number and depends on the symmetry point group of the molecule. HBTP belongs to  $D_{3h}$ , resulting in  $\gamma=6$ .  $I_1$ ,  $I_2$ , and  $I_3$  were obtained from the optimized geometry of an isolated HBTP molecule. For the numerical evaluation a temperature of  $T=298 \text{ K}$  was used, resulting in  $S_{\text{rot(sol)}} = \Delta S_{\text{rot}} = -150.6 \text{ J}\cdot\text{mol}^{-1}\cdot\text{K}^{-1}$ .

## 4 Density Functional Theory

### 4.1 Computational Details

Initially, a free standing HBTP monolayer was simulated and optimized with the Quantum ESPRESSO program,<sup>5</sup> using two density functional theory (DFT) based approaches: **(I)** a GGA-PBE functional<sup>6</sup> with an empirical dispersion correction (D2) proposed by Grimme (PBE+D),<sup>7</sup> and **(II)** a van der Waals density functional (vdW-DF).<sup>8</sup> All DFT calculations were conducted with periodic boundary conditions. The accuracy of DFT derived energies for halogen bonds was first tested against higher level calculations: the PBE+D binding energy of a Br $\cdots$ N halogen bond in a pyridine-bromobenzene dimer (-11.4 kJ/mol) was very similar to the value obtained using MP2 (-8.9 kJ/mol) and to a published CCSD(T) value (-9.1 kJ/mol).<sup>9</sup> The structure was constrained to a hexagonal lattice, but no further symmetry constraints were applied. The energetic minimum for a free standing HBTP monolayer was found for a lattice parameter of  $A = B = (12.48 \pm 0.01) \text{ \AA}$ ,  $\gamma = 120^\circ$  (PBE+D calculations) and  $A = B = (12.50 \pm 0.05) \text{ \AA}$ ,  $\gamma = 120^\circ$  (vdW-DF calculations). The binding energy per molecule with respect to vacuum corresponds to -45.5 kJ/mol (PBE+D) or -48.3 kJ/mol (vdW-DF).

The underlying graphite was included in further calculations to estimate the total binding energy of HBTP in the adsorbed monolayer. In the first step a free standing HBTP monolayer was optimized with its lattice parameters constrained to the commensurate superstructure, i.e.  $A = B = 5 \times a_{\text{graphite}} = 12.32 \text{ \AA}$  and  $\gamma = 120^\circ$ . This optimized HBTP structure was then adsorbed on a two layer graphite slab such that the positions of the HBTP triphenylene cores mimic the Bernal stacking of graphite. For the final optimization of the combined system only the atomic coordinates of the lower graphite layer were fixed, while all atoms of the HBTP monolayer were free to relax laterally and vertically. However, there was no substantial lateral relaxation,

indicating either a relatively flat potential energy hypersurface or that this configuration already corresponds to an energy minimum.

The total binding energy of HBTP in the adsorbed monolayer on graphite including molecule-molecule and molecule-surface interactions was calculated as:

$$\Delta H_{\text{mono}} = E_{\text{graphite+monolayer}} - E_{\text{graphite}} - E_{\text{molecule}} = -229.6 \text{ kJ/mol}$$

The adsorption energy of HBTP on graphite, i.e. the contribution of molecule-surface interactions, was calculated as:

$$E_{\text{ads}} = E_{\text{graphite+monolayer}} - E_{\text{graphite}} - E_{\text{monolayer}} = -186.1 \text{ kJ/mol}$$

( $E_{\text{molecule}}$  corresponds to the energy of a single isolated HBTP molecule in the gas phase;  $E_{\text{graphite+monolayer}} / E_{\text{monolayer}}$  and  $E_{\text{graphite}}$  are referred to one HBTP unit cell and 5×5 graphite unit cells, respectively)

## 4.2 Additional results

---

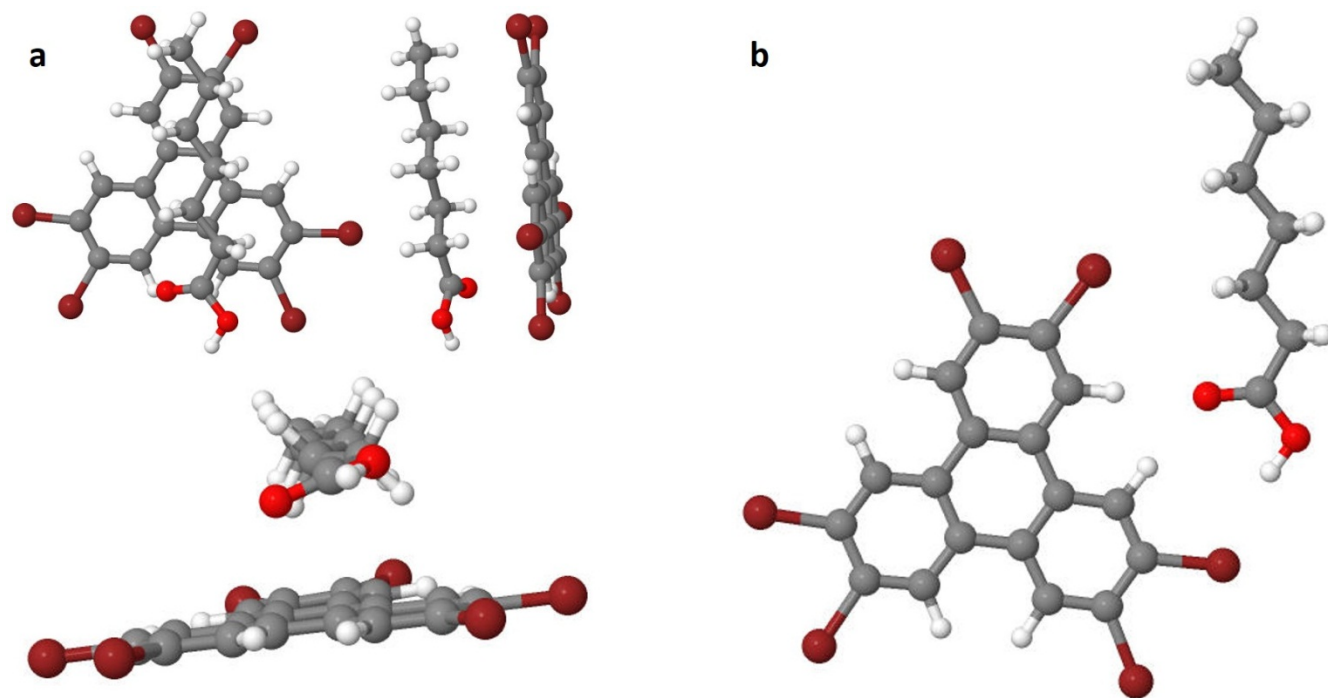


**Fig. S3.** Optimized structures of 7A + HBTP aggregates simulated with periodic boundary conditions using a  $22 \times 22 \times 22 \text{ \AA}^3$  large super-cell. These simulations were carried out to estimate the strength of solute-solvent interactions for a semi-quantitative comparison to solvent-solvent interactions. (a) different views of a configuration with 7A on top of HBTP; binding energy:  $-49.8 \text{ kJ/mol}$ . (b) configuration with 7A attached sidewisely to HBTP through the combination of hydrogen bonds: 7A-carbonyl  $\cdots$  HBTP-hydrogen and 7A-hydroxyl  $\cdots$  HBTP-bromine; binding energy:  $-34.1 \text{ kJ/mol}$ .

---

## 5 References

1. R. Gutzler, W. M. Heckl and M. Lackinger, *Rev. Sci. Instrum.*, 2010, **81**, 015108.
2. M. Mammen, E. I. Shakhnovich, J. M. Deutch and G. M. Whitesides, *J. Org. Chem.*, 1998, **63**, 3821-3830.
3. W. Song, N. Martsinovich, W. M. Heckl and M. Lackinger, *J. Am. Chem. Soc.*, 2013, **135**, 14854-14862.
4. W. Song, N. Martsinovich, W. M. Heckl and M. Lackinger, *Phys. Chem. Chem. Phys.*, 2014, **16**, 13239-13247.
5. P. Giannozzi, S. Baroni, N. Bonini, M. Calandra, R. Car, C. Cavazzoni, D. Ceresoli, G. L. Chiarotti, M. Cococcioni and I. Dabo, *J. Phys. - Condens. Mat.*, 2009, **21**, 395502.
6. J. P. Perdew, K. Burke and M. Ernzerhof, *Phys. Rev. Lett.*, 1996, **77**, 3865.
7. S. Grimme, *J. Comput. Chem.*, 2006, **27**, 1787-1799.
8. K. Lee, E. D. Murray, L. Kong, B. I. Lundqvist, and D. C. Langreth, *Phys. Rev. B* 2010, **82**, 081101.
9. S. Tsuzuki, A. Wakisaka, T. Ono and T. Sonoda, *Chem. Eur. J.*, 2012, **18**, 951-960.